RSC Advances

ROYAL SOCIETY
OF **CHEMISTRY**

www.rsc.org/advances

Astrogliosis in a Dish: Substrate Stiffness Induces Astrogliosis in Primary Rat Astrocytes

Christina L. Wilson[1], Stephen L. Hayward[1], and Srivatsan Kidambi[1,2,3,4,5,*]

[1]Department of Chemical and Biomolecular Engineering,

820 N 16th Street, 207 Othmer Hall, University of Nebraska-Lincoln, NE, 68588

[2]Nebraska Center for Materials and Nanoscience,

855 N 16th St, Lincoln, University of Nebraska-Lincoln, NE, 68588

[3]Nebraska Center for the Prevention of Obesity Diseases,

316C Leverton Hall, 1700 35th Street, University of Nebraska-Lincoln, NE, 68583

[4]Mary and Dick Holland Regenerative Medicine Program,

42nd and Emile Street, University of Nebraska Medical Center, Omaha, NE, 68198.

[5]Fred & Pamela Buffett Cancer Center,

University of Nebraska Medical Center, Omaha NE, 68198.

[*]indicates corresponding author.

Srivatsan Kidambi
Department of Chemical and Biomolecular Engineering
University of Nebraska-Lincoln
820 N 16 Street, 207 Othmer Hall, Lincoln NE 68588
Ph: 402-472-4443
Email: skidambi2@unl.edu

ABSTRACT

Astrogliosis due to brain injury or disease can lead to varying molecular and morphological changes in astrocytes. Magnetic resonance elastography and ultrasound have demonstrated that brain stiffness varies with age and disease state. However, there is a lack in understanding the role of varied stiffness on the progression of astrogliosis highlighting a critical need to engineer *in vitro* models that mimic disease stages. Such models need to incorporate the dynamic changes in brain microenvironment including the stiffness changes. In this study we developed a polydimethyl siloxane (PDMS) based platform that modeled the physiologically relevant stiffness of brain in both a healthy (200 Pa) and diseased (8000 Pa) state to investigate the effect of stiffness on astrocyte function. We observed that astrocytes grown on soft substrates displayed a consistently more quiescent phenotype while those on stiff substrates displayed astrogliosis-like morphology. In addition to morphological changes, astrocytes cultured on stiff substrates demonstrated significant increase in other astrogliosis hallmarks- cellular proliferation and glial fibrillary acidic protein (GFAP) protein expression. Furthermore, culturing astrocytes on stiff surface resulted in increased reactive oxygen species (ROS) production, increased super oxide dismutase activity and decreased glutamate uptake. Our platform lends itself for study of potential therapeutic strategies for brain injury focusing on the intricate brain microenvironment-astrocytes signaling pathways.

INTRODUCTION

The brain is a mechanically heterogeneous organ that utilizes endogenous mechanical forces to regulate aspects of tissue and cellular function. Magnetic resonance elastography, ultrasound and mechanical compression techniques have demonstrated that stiffness of brain regions vary [1, 2] and these mechanical properties substantially change with age and disease state [3-7]. Although endogenous micromechanical energy is important for normal brain function, substantially greater mechanical forces acting on the brain can result in loss of consciousness, irreversible cognitive dysfunction, progressive neurodegeneration and even death [8-10]. Numerous studies have focused on the deleterious consequences of brain injury and disease, however, the host of deleterious molecular signaling pathways triggered as cellular-mechanical consequences of head trauma and the underlying mechanisms of these injuries are still not clear. Several studies have demonstrated that the mechanical microenvironment of a cell influences key aspects of cell functionality and structure [11-16]. Hence, it is critical to investigate the role of varied stiffness on cellular function.

The classically accepted paradigm regards neurons as the major player associated with brain function in normal and diseased states. Astrocytes - the most abundant cell type in the brain - have largely been considered as supporting cells for neurons that provide an ideal environment for neuronal-cell function but have no direct role in brain activity. However, accumulating evidence has challenged this paradigm to suggest that astrocytes are sophisticated participants in a diverse variety of functions for normal brain development and activity [17-21]. Studies have also implicated astrocytes to play an important role in the progression of several neurodegenerative diseases, including,

Alzheimer's disease (AD), Parkinson' disease, Down Syndrome, Amyotrophic lateral sclerosis and epilepsy [22-26]. Astrogliosis/reactive astrocytosis is marked by an abnormal increase in the number of astrocytes frequently observed in brain trauma, infection, stroke, and neurodegenerative diseases [27]. This process involves activation of astrocytes leading to production of proinflammatory mediators such as cytokines, chemokines, glutamate, reactive oxygen species (ROS), and prostanoids [28, 29]. During astrogliosis, astrocytes become hypertrophic with upregulated expression of intermediate filaments (e.g. glial fibrillary acidic protein (GFAP), vimentin), oxidative stress markers, and cytokines. Advanced astrogliosis ultimately leads to formation of glial scar as a physical barrier, which can inhibit axonal regeneration [30]. Reactive astrocytosis is not merely a marker for neuropathology, but plays an essential role in orchestrating injury response, regulating inflammation and overall tissue repair that markedly impacts functional and clinical outcomes. While there has been reasonable progress toward understanding astrocyte physiology, little is known about the effect of changes in brain microenvironment, including stiffness, in mediating astrogliosis.

In our study, we utilized a polydimethyl siloxane (PDMS) based substrate with tunable stiffness to study the effect of various degrees of stiffness on the phenotype of primary rat cortical astrocytes. Our working hypothesis is that variation in matrix stiffness will influence astrocyte phenotype and function, and that astrocytes will subsequently develop astrogliosis-like responses to mechanical perturbation. We employed a soft substrate (200 Pa) to represent healthy brain tissue and stiff substrate (8000 Pa) to represent diseased brain tissue as these fall in the range of previous *in vivo* and *in vitro* investigations into brain stiffness and the effect of changing brain stiffness [2, 3, 31-33]. We

studied the effect of stiffness on commonly accepted hallmarks of astrogliosis including changes in cell morphology, proliferation, expression of vimentin and GFAP. Further we characterized the effect of stiffness on glutamate uptake, an important function of astrocytes, and perturbation of cellular oxidative state induced by the surface stiffness. Our observations indicate a strong dependence of primary astrocytes function on the culture substrate stiffness thus demonstrating a potential pathway for the progression of astrogliosis.

MATERIALS AND METHODS

Substrate Characterization

CytoSoft® 6-well plates of stiffness measured to be elastic modulus 200 Pa and 8000 Pa were purchased from Advanced BioMatrix. Extensive property testing was performed by Advanced BioMatrix to assure the quality of surfaces. Surfaces were coated with poly-L-lysine (PLL) prior to cell seeding according to manufacturer instructions. Florescent images of carboxyfluorescein treated PLL surfaces (N = 3) were imaged and the fluorescence intensity quantified by Image J Analysis Software [NIH] to demonstrate the uniformity of substrate coating is not varied by substrate stiffness.

Isolation and Culture Of Primary Astrocytes

This study was carried out in strict accordance with the recommendations in the Guide for the Care and Use of Laboratory Animals of the National Institutes of Health. The protocol was approved by the Committee on the Ethics of Animal Experiments of the University of Nebraska-Lincoln (Project ID: 1046). Primary cortical astrocytes were prepared from 1-3 day-old Sprague-Dawley rat pups [Charles River] in compliance with UNL's IACUC protocol 1046 and according to protocol with slight modifications [34, 35]. In

short, the tissue was dissociated with 0.025% Trypsin [Life Technologies] and 0.0016% DNase [Roche] which was quenched by serum containing media (DMEM [MP Biomedicals], 10% Fetal Bovine Serum [Atlanta Biologicals], and 1% penicillin-streptomycin [Life Technologies]). The trypsin was removed by centrifugation at 1700 rpm for 5 min after which the pellet was suspended in media and gently homogenized with glass pipette. The homogenate was then passed through a 70µm cell filter, pelleted, suspended in media and seeded on tissue culture petri dish. On day *in vitro* (DIV) two the petri dish was vigorously shaken to remove loosely attached cells, mostly neurons and microglia, and media was exchanged for fresh media. The vigorous shaking was repeated prior to each media change and passaging to remove any remaining loosely attached cells, including microglia. This method is used to remove contaminating glia from primary mixed cultures as described in Tamashiro et al and Cole et al [36, 37]. Cultures were characterized by fluorescent microscopy using anti-glial fibrillary acidic protein (GFAP) [DAKO] and 4',6-diamidino-2-phenylindole (DAPI) nuclear stain [Thermo Scientific] yielding cultures of >90% GFAP positive cells (Supplementary Figure 3) .

Experimental Culture

Astrocytes received media changes every three days until 70-80% confluent (DIV 6) at which point the cells were passaged by dissociation with 0.05% Trypsin-EDTA [Life Tech], quenched with culture media, pelleted, suspended in culture media and seeded in tissue culture dish at three million cells per dish. Cultures were allowed to expand with media changed every three days until confluent two times. Passage three

astrocytes were seeded for experiments on PLL coated CytoSoft® 6-well plates of stiffness measured to be 200 Pa and 8000 Pa [Advanced BioMatrix].

Phase Images

Phase images were obtained for morphology of live cells assessment using an Axiovert 40 CFL [Zeiss] and Progres C3 [Jenoptick] camera.

Actin Staining, Cell Size And Circularity

Cells were fixed with 4% paraformaldehyde in PBS at room temperature for 20 min. Samples were permeabilized in 2% Triton X-100 for 15 min at room temperature. Actin 488 ready Probe [Life Technology] was applied according to manufacturer instructions and incubated on fixed cells at room temperature for 30 min. Nuclei were visualized with DAPI stain by a 5 min incubation at room temperature in a 1 µg/ml solution. Images were obtained using Axiovert 40 CFL [Zeiss] and a Progres C3 [Jenoptick] camera with an X-Cite series 120Q [Lumen Dynamics] lamp utilizing FITC or DAPI filter [Chroma]. Actin images were assessed for average cell area and circularity utilizing the measure feature of NIH Image J. Ten random cells per image were highlighted and quantified for cell area and circularity. Cell area was reported as a fraction of the average cell size on 200 Pa surface. Cell circularity was reported in arbitrary units between 0 and 1 with a perfect circle ranking 1.

Western Blot

Whole cell lysates were collected using a RIPA buffer (PBS, pH 7.4, 1% CA 630 IGEPAL, 0.5% deoxycholate, 0.1% sodium dodecyl sulfate, protease inhibitor cocktail and phenylmethylsufonyl fluoride) [Sigma Aldrich]. Proteins were quantified using

coomassie blue [Thermo Scientific Kit 23200]. 10-50 µg of total protein was separated by 10% SDS-polyacrylamide gel electrophoresis and transferred to Immobilon FL membrane [Millipore] using transfer buffer (25 mM Tris, 192 mM glycine, 10% methanol) and detected with primary antibodies (GAPDH [Millipore], GFAP [DAKO], EAAT1 [Abcam], EAAT2 [Abcam] and Vimentin [GeneTex]) followed by Dylight 800 polyclonal secondary antibody [Thermo Scientific] and imaged with an Odyssey FC [LiCor].

BrdU Staining

Proliferation was assessed utilizing 5-Bromo-2-Deoxyuridine (BrdU) which incorporates into newly formed DNA during proliferation and is then detectable by Alexa Fluor 488 conjugated antibody [Life Technology]. This was performed by first incubating the astrocyte monolayer in 10 µM BrdU in culture media solution for 24 hr at 37° C prior to fixing the cells in a suspension of 4% paraformaldehyde. The cells were permeabilized with 0.1% Triton X-100 in PBS, DNA denatured with 0.03% DNase in PBS, and blocked with 1% BSA in PBS. Finally, the BrdU was detected by incubating the cells in anti-BrdU antibody [Life Technology] in 1% BSA in PBS overnight at 4° C, washed two times in 1x PBS and florescence intensity quantified by FACS Cantoll (BD) in the green channel (ex. 495, em. 520; 100,000 total events/read) against cells not treated with BrdU.

ROS Generation

5-(and-6)-chloromethyl-2′,7′-dichlorodihydrofluorescein diacetate (CM-H$_2$DCFDA) is a fluorescent indicator activated by the presence of ROS. The intensity of CM-H$_2$DCFDA was quantified using a FACS Cantoll (BD). Culture media was aspirated and the cells washed with warm PBS. 10 µM CM-H$_2$DCFDA [Life Technologies] in DMEM was added to each well and incubated at 37° C for 30 min. Cells were washed three times with

PBS, trypsinized, transferred to DMEM in flow cytometry tubes and analyzed for fluorescence in the green channel (ex. 495, em. 520; 100,000 total events/read) against cells not treated with CM-H$_2$DCFDA.

Superoxide Dismutase Activity

The activity of CuZnSOD was measured by in gel reduction of nitroblue tetrazolium method described in Natarajan et al with some modifications [38]. First, proteins were lysed in a buffer consisting of 50 mM Nacl, 5 mM EDTA, 0.1% Triton X-100 and protease inhibitor. Next the protein was quantified by BCA assay and samples containing 30 µg protein made with loading dye consisting of 25 mM Tris-HCL (6.8), 50% glycerol, 0.5% Bromophenol blue. A 12% bis-acrylamide gel without SDS was utilized with a running buffer consisting of 0.2 M glycine, 0.02 M Trizma and 0.01 M EDTA. After samples were separated by gel electrophoresis the gel was removed and incubated for 30 min in staining solution (0.05 M K$_2$HPO$_4$, 0.005 M KH$_2$PO$_4$, 0.16 mM nitroblue tetrazolium, 0.26 mM riboflavin and 0.1% TEMED). The gel was then washed, suspended in DI water and incubated in ambient light overnight. Images were obtained utilizing Quantity One Analysis Software [Biorad] and quantified via Studiolite [Lycor].

Glutamate Uptake

The uptake of [3H] glutamic acid was used to determine change in glutamate uptake experienced by astrocytes on soft and stiff surface. The media was removed and replaced by serum free high glucose DMEM containing 50 µM glutamate and 18.5 kBq of [3H] glutamic acid [Perkin Elmer] which was allowed to incubate at 37° C of 15 min. Uptake was terminated by removal of working solution and cells washed twice with ice-cold PBS lysed in 10 mM NaOH containing 0.1% Triton X-100. 300 µl of lysate was

added to liquid scintillation cocktail [Fisher Scientific] and quantified by counting. The protein content was assayed using Bradford assay [Thermo Scientific Kit 23200]. Results were reported as CPM/ μg protein.

Gene Expression

Total RNA expression was quantified by quantitative real time PCR as described previously [39]. Primers were obtained from Integrated NDA Technologies [Coralville, IA] of the following sequences: Vimentin (forward 5′-GACAATGCGTCTCTGGCACGTCTT-3′ and reverse 5′-TCCTCCGCCTCCTGCAGGTTCTT-3′), GLAST (forward 5′-CTACTCACCGTCAGCGCTGT-3′ and reverse 5′-AGCACAAATCTGGTGATGCG-3′) and GLT1 (forward 5′-CCCAAGTACGAAGGGACAATTA-3′ and reverse 5′-CTCATCCACAGTCCACATCTTC-3′). Expressions were found relative to housekeeping gene GAPDH (forward 5′-ATGATTCTACCCACGGCAAG-3′ and reverse 5′-CTGGAAGATGGTGATGGGTT-3′) utilizing the ΔΔCT method. Final results were reported as normalized to the average relative expression on the soft surface.

Statistical Analysis

All data is presented as the mean ± the standard deviation. Statistical comparisons between treatments utilized Sigma Plot Student T-Test and pool size as indicated. For data, which did not follow a gaussian distribution, a Mann-Whitney rank test was employed with pool size as indicated.

RESULTS

Stiffness Induces Astrogliotic Morphology And Actin Stress Fibers

To determine if altering the physical stress experienced on the cellular level could induce an astrogliosis-like morphology, we isolated primary astrocytes and cultured the

cells on PLL coated PDMS substrates of varied stiffness (**Figure 1**). We observed at 72

hr primary astrocytes displayed smaller, rounded morphology on 200 Pa (soft)

substrates and larger, elongated morphology on 8000 Pa (stiff) substrates (**Figure 1**).

The morphology in stiffer substrate is akin to the astrocytes morphology observed *in*

vivo during astrogliosis [27] with more process extensions and increased surface area. To

assure that this observed phenomena was not a result of heterogeneous PLL coating,

we measured the fluorescent intensity of adsorbed carboxyfluorescein on PLL coated

soft and stiff surfaces and found surface coating uniformity on both substrates

(**Supplemental Figure 1**). We further investigated the effect of stiffness on cell

morphology by immunostaining the actin cytoskeletal structure (**Figure 2A**). Similar to

the phase images, astrocytes on 200 Pa substrates had a rounded morphology with

smaller cell bodies while the morphology substantially changed when cultured on 8000

Pa substrates possessing larger cell bodies and stretched morphology. Quantification

revealed the average cell size on the stiff surface covered 1.6 ± 0.4 times the surface

area of the average cell cultured on the soft surface (**Figure 2B**). Furthermore cells on

the soft surface had a circularity rank of 0.43 ± 0.09 while cells on the stiff surface has a

circularity rank of 0.21 ± 0.04, quantifying that astrocytes on the soft surface had

rounded morphology (**Figure 2C**). This observation is similar to other studies that have

demonstrated astrocytes were less branched, more rounded and had quiescent

morphology on surfaces between 100 and 300 Pa while astrocytes had more branching,

covering more surface area on surfaces greater than 1000 Pa [33, 40, 41]. We also

observed a dramatic increase in actin organization and cell polarizability on stiffer (8000

Pa) surfaces. This has been observed in other cells and is generally known as actomyosin bundles or stress fibers [42-44].

Stiffness Increases Astrocytes Proliferation

Studies have demonstrated that astrogliosis results in the increase of astrocytes present in damaged areas by induction of astrocyte proliferation [27]. We investigated the effect of stiffness on astrocytes proliferation on soft (200 Pa) and stiff (8000 Pa) substrates using BrdU staining (**Figure 3A**). We observed that astrocytes on stiff substrates had a 1.7 fold increase ($P < 0.05$) in BrdU staining compared to those on soft substrates after 72 hours in culture. In our study we utilized Brdu assay and flow cytometry to quantify the phenotypic change independent of cell number. BrdU assay measured the incorporation of BrdU in replicating DNA early in mitotic cell cycle due to proliferation and flow cytometry allowed for the quantification on a per cell basis evaluating the average florescent intensity of 10,000 cells. Therefore our data demonstrated that the changes in brain stiffness might be one of the potential causes for the increase in astrocytes during brain injury.

Stiffness Induces Up-regulation of GFAP Expression

We next investigated the effect of stiffness on GFAP protein expression, an intermediate filament expressed exclusively by astrocytes. Increase in GFAP protein expression is a clinical hallmark sign of astrogliosis both *in vivo* and *in vitro* [27, 45]. A 1.3 fold up-regulation ($P < 0.05$) in GFAP protein expression (**Figure 3B**) was observed in astrocytes cultured on stiff substrates (8000 Pa) compared to soft substrates (200 Pa). Further, we probed the effect of stiffness on the protein expression of a less recognized intermediate gliofilament, vimentin, which has also been observed to increase in

astrogliosis and found no up-regulation in protein expression (**Figure 3B**) in primary

astrocytes cultured on stiff substrates compared to soft substrates. As gene expression

proceeds protein expression, and can be used as an early indication of phenotypic

change, to further probe the vimentin expression RT-PCR was utilized to quantify gene

expression [46-48]. It was observed that vimentin gene expression (**Supplemental Figure**

2) was up-regulated 1.6 fold (P < 0.05) indicating a temporally sensitive effect of

substrate stiffness on vimentin expression. Although increase in GFAP and vimentin

expression have been extensively used as astrogliosis markers *in vivo* and *in vitro,*

studies in vimentin knock-out mice have shown that vimentin up-regulation is not

required for induction of astrogliosis [49]. This observation, in combination with the

previous results, supports our hypothesis that astrocytes cultured in environment with

increased stiffness induce astrogliosis *in vitro*.

Stiffness Increases ROS Production And SOD Activity In Primary Astrocytes

Animals and other experimental models have demonstrated that specific signaling

cascades including production and release of toxic levels of ROS might stimulate

astrogliosis [50-52]. Utilizing H_2DCFDA and flow cytometry we quantified the effect of

stiffness on generation of intercellular levels of ROS when primary astrocytes were

cultured in either a healthy or a stiff diseased-like environment (**Figure 4A**). A 9-fold

increase (P < 0.001) in intercellular ROS production was observed in astrocytes

cultured on stiff substrates compared to soft substrates. This is a significant finding as

animal   studies   have   demonstrated   that   chronic   neuorinflammation   and

neurodegeneration associated with massive/prolong brain injury or astrocyte stress

leads to amplification of a microglia-astrocyte crosstalk and uncontrolled release of ROS

[50-52]. Our model demonstrates that primary astrocytes cultured on stiffer substrate experience increase in ROS levels similar to the transition observed in the animal injury models.

The uncontrolled increase in ROS can lead to oxidative stress and cellular damage if not countered by the activity of endogenous anti-oxidant species as has been seen in a number of toxicology and neurodegenerative disease studies [38, 53, 54]. Copper-Zinc super oxide dismutase (CuZnSOD) is an endogenous anti-oxidant which targets the reduction of super oxide species into peroxide to alleviate oxygen radicals and protect the cell from oxidative stress [55]. The CuZnSOD activity was measured (**Figure 4B**) utilizing an in gel NBT reduction assay and found to be increased by 1.5 fold ($P < 0.05$) in astrocytes cultured on the 8000 Pa surface compared to the astrocytes on 200 Pa PDMS. These result demonstrate the ability of this model to follow the adaptive oxidative state pathways of reactive astrocytes which could increase understanding of the astrogliotic phenotype and uncover potential therapeutic methods.

Stiffness Induces Loss In Glutamate Uptake In Primary Astrocytes

Glutamate uptake is a paramount function of astrocytes in proper brain activity. Consequently, we investigated the effect of stiffness induced astrogliosis phenotype on the regulation of the glutamate uptake mechanism in astrocytes (**Figure 5**). We first quantified the overall functionality of glutamate transport and observed a 2-fold decrease ($P < 0.05$) in glutamate uptake in primary astrocytes cultured on stiff substrates compared to those on soft. To elicit the cause of glutamate uptake loss, we next quantified the gene and protein expression of key glutamate transporters in relation to substrate stiffness. Five subtypes of glutamate transporters have been identified in

rodents and humans including Glutamate/Asparate transporter (GLAST) and Glutamate Transporter 1 (GLT1) as the transporters predominately expressed in astrocytes and required for regulating the glutamate uptake in the brain [56]. Therefore, we quantified the relative GLAST and GLT1 gene expression following culture on soft and stiff surfaces as changes in gene expression may be an early indication of transporter protein alteration. Although GLAST expression remained similar on the varied surfaces, GLT1 expression was significantly increased (1.4 fold, $P < 0.05$) on the 8000 Pa surface (**Figure 5B**). Furthermore, we quantified GLT1 and GLAST protein expression to indicate if the change in gene expression was followed similarly to the change in protein expression. The quantification of protein expression indicated no change in GLT1 or GLAST protein expression (**Figure 5C**) confirming that the alteration in glutamate uptake was not a result of altered transporter expression resulting from culture surface stiffness. This data is useful to provide insight to the current pool of understanding on glutamate homeostasis and variation in tissue stiffness.

DISCUSSION

Astrogliosis/reactive astrocytes are a prominent and ubiquitous reaction of astrocytes to many forms of brain injury, often implicated in the poor regenerative capacity of the central nervous system (CNS). Reactive astrogliosis is associated with new gene expression or up-regulation of molecules that are at low levels in quiescent astrocytes [27, 57, 58]. However, little is known about the structural and molecular mechanisms underlying the transformation of astrocytes to the reactive state. Furthermore, there are currently no comprehensive profiles of brain injury-initiated protein changes in reactive astrocytes.

Animal models such as stab wound-induced brain injury, neurotoxic lesions, genetic diseases (twitcher mouse) and inflammatory demyelination (experimental allergic encephalomyelitis) have been extensively used to investigate the progression of astrogliosis [59]. However, *in vivo* models have numerous drawbacks including: (1) the challenge associated with mechanistic study of reactive astrogliosis induction, (2) difficulties in reproducing the same extent of injuries in multiple experiments, (3) interference of systemic response to trauma in specific cellular effect and (4) inability to identify biochemical properties of reactive astrocytes [60].

In vitro models allow the investigation of an isolated phenomenon in a well-defined environment, which is free from complex cellular interactions. Established astrogliosis *in vitro* models include *in vitro* mechanical injury model (e.g. scratch wound, platform stretch)[61, 62], low temperature trauma model [63], and addition of growth factors to astrocyte cultures [64, 65]. However, these methods result in heterogeneous population of injured and uninjured cells resulting in varying gene and protein expression changes in astrocytes. Furthermore, these models do not facilitate the understanding of the molecular and cellular properties of astrocytes resulting from extended, static mechanical change in brain microenvironment, such as that resulting from swelling or change in microenvironment composition, and how they regulate the functional astrocytes. There is a critical need for an *in vitro* injury model to be able to investigate the molecular changes in astrocytes systematically and quantitatively in a reproducible manner.

In this study we utilized a PDMS based platform to investigate the effect of stiffness on primary astrocyte function. This approach has several advantages over the previously

mentioned methods including ease of replication, uniformity of injury and ability to mimic mechanical properties of brain microenvironment in different disease states. PDMS is a biocompatible, stable and tunable material which provides a platform with uniform mechanical properties. The uniform mechanical properties induces a homogeneous population of "injured" cells which can be assessed for molecular changes resulting from mechanical stiffness. PDMS is chemically inert but can be uniformly modified with PLL, a standard culture dish coating for neural cells, to facilitate astrocyte attachment. This allows for a uniform chemical coating which assures that change in cellular phenotype is solely the result of platform mechanical stiffness.

We employed a soft substrate (200 Pa) to represent healthy brain tissue and stiff substrate (8000 Pa) to represent diseased brain tissue. These values were chosen due to the following reasoning: 1) the elastic modulus of healthy rat and porcine brain has been measured via indentation techniques and found to fall in the range of 100 to 400 Pa,[31, 66] and 2) it has been suggested that the changes in local mechanical properties may play a role in disease pathology, thus we utilized a PDMS platform of greater stiffness (8000 Pa) to determine if altering the physical forces on the cellular level solely prompts the onset of astrogliosis. Although tissue maturity and some neurodegenerative diseases have been shown to decrease the overall tissue stiffness several injury and disease states, such as metastatic tumor, stroke and traumatic brain injury, have been observed to significantly increase tissue stiffness [3, 4, 7, 67-69].

The successful induction of astrogliotic phenotype by this model serves to provide preliminary information on the phenotypic changes of astrocytes due to local alteration of microenvironmental stiffness *in vitro*. We observed that astrocytes grown on soft

substrates displayed a consistently more quiescent phenotype while those on stiff substrates displayed astrogliosis-like phenotype. Georges and coworkers demonstrated that neurons have consistent actomysin formation regardless of surface stiffness while astrocytes demonstrated mechanosensitivity by increased polarization on stiff surfaces [33]. Prager-Khoutorsky and coworkers demonstrated that human fibroblasts also showed similar changes in morphology possessing smaller, rounded morphology in soft substrates and elongated morphology with large focal adhesion points in stiff substrates [70]. Overall our data supports the hypothesis that reactive morphology is induced by increased surface stiffness.

Primary astrocytes cultured on stiff substrates demonstrated significant increase in common hallmarks for astrogliosis- glial fibrillary acidic protein (GFAP) protein expression and proliferation. Previous studies have shown that astrocytes devoid of GFAP expression are unable to accomplish the reactive phenotype in injury and disease [45, 71]. This is the first stiffness induced astrogliosis model to quantify a cellular increase in GFAP protein expression although stretch, hyperthermia and chemically induced models of astrogliosis have all observed similar up-regulation post injury [62, 63, 72]. Previous mechanical models have utilized GFAP staining to identify astrocyte populations and quantify cell numbers on soft and stiff polyacrylamide (PA) gels but have not quantified protein expression. These studies utilized GFAP staining to indicate an increased presence of astrocytes on stiff surfaces attributing this to difficulty of astrocytes to attach and grow on soft polyacrylamide (PA) gels [33, 73]. Georges et al quantified the difference in adhesion by counting the number of cells attached to soft (200 Pa) and stiff (9000 Pa) surfaces at 4 and 24 hr of culture. They noted a slightly

higher number of astrocytes at 4 hr compared to 24 hr suggesting a time dependent cell detachment from the soft surfaces not observed on stiff surfaces [33]. Furthermore, Jiang and coworkers quantified the number of mature astrocytes attached to soft (300 Pa) vs stiff (27 and 230 kPa) PA gels by counting GFAP positive astrocytes and found a significantly higher number of adherent astrocytes on stiff PA gels [73]. Our results suggest that an increase in astrocyte number in our model on stiff surfaces is dependent on induction of proliferation by the per cell analysis of Brdu incorporation in astrocyte DNA. Our observations support the hypothesis that the increase in culture surface stiffness induces a reactive phenotype in astrocytes.

Our study observed that astrocytes on stiff disease-like surface also resulted in increased ROS production and anti-oxidant CuZnSOD activity. This is akin to the observation in animal studies that have demonstrated chronic neuorinflammation and neurodegeneration associated with massive/prolong brain injury or astrocyte stress leading to uncontrolled release of ROS [50-52]. Further, Superoxide Dismutase (SOD) is an anti-oxidative species in eukaryotic cells which convert superoxide radicals into hydrogen peroxide to prevent oxidative stress and damage in the presence of increased ROS generation. The most important parameter determining biological impact of SOD is the enzyme anti-oxidant activity with Copper-Zinc SOD (CuZnSOD) constituting approximate 90% of all SOD activity in eukaryotic cells [55]. Our results show that reactive astrocytes induced by mechanical stiffness experience an increase in ROS generation and increase in CuZnSOD activity suggesting that the oxidative state of reactive astrocytes is changed from those of quiescent astrocytes as they adapt to the increased stress from varied microenvironment. To our knowledge, no study has specifically

investigated and demonstrated a role of stiffness in regulation of ROS levels in astrocytes. Since varied oxidative state is a commonly observed mechanism in disease these results indicate our platform lends itself for investigation of potential therapeutic strategies manipulating oxidative state during brain injury focusing on the intricate brain microenvironment-astrocytes signaling pathways.

Previtera and coworkers demonstrated that the global glutamate concentration of mixed cultures do not change between soft and stiff surfaces when the ratio of neurons to astrocytes were similar however when the ratio of neurons was higher than that of astrocytes the global concentration of glutamate increased suggesting that the number of astrocytes is key to the global concentration of glutamate [74]. Jiang and coworkers showed that neurons in mixed cultures were much less susceptible to excitotoxicity on stiffer gels [73]. This resistance is attributed to an increased number of astrocytes on the stiff environment compared to softer substrates. Our results are in agreement with these studies and provide insight that increased number of astrocytes may be needed to prevent glutamate toxicity as the capacity of individual astrocytes to uptake glutamate is decreased on stiff surfaces. Furthermore, to probe why there is an observed loss in glutamate uptake we quantified the gene expression of glutamate transporters. Our results observed no change in GLAST expression and a significant increase in GLT1 gene expression on the stiff surface suggesting that the loss in function is not a result of decreased gene expression. Furthermore, GLAST and GLT1 protein expression was unchanged on the 8000 Pa surface compared to the 200 Pa surface. This indicates that the loss in glutamate uptake is unrelated to the amount of glutamate transporters expressed and therefore must lie in some other mechanism. To uncover the root of

glutamate homeostasis perturbation it would be beneficial to observe other factors influencing transporter function, energy metabolism and mitochondrial health. This may be an informative future work of mechanistic discovery utilizing this platform but is beyond the scope of the current work. In the current study, we have demonstrated the potential of our *in vitro* platform to emulate the onset of astrogliosis by modeling the stiffness of brain in healthy and injury state. Our platform recreates astrogliosis *in vitro* by inducing cellular adaptation to increasing microenvironment stiffness. This model can be used to facilitate understanding the role of complex cell-microenvironment interactions that are hard to dissect in clinical conditions of brain injury and neurodegenerative diseases.

In summary (**Figure 6**), we demonstrated an innovative approach to model astrogliosis on tunable substrates that recreate the varying stiffness in brain mimicking healthy and diseased state. This approach has several advantages over the method used by other group including high fidelity, ease of duplication, biocompatibility and ability to mimic brain microenvironment in different disease states. We have provided evidence that our platform emulates the various clinical markers of astrogliosis by modulating the stiffness of the substrate to correlate with normal (200 Pa) and injury (8000 Pa) conditions of brain microenvironment. To validate the mimicry of the clinical conditions, we observed that astrocytes grown on the healthy brain stiffness (200 Pa) displayed a consistently more quiescent morphology as compared to astrocytes cultured on stiff substrate (8000 Pa) that displayed reactive morphology. Furthermore, we also demonstrated that our model captured the changes in proliferation and GFAP protein expression, clinical hallmarks for astrogliosis. We demonstrated that astrocytes cultured on stiffer

environment resulted in increased ROS levels, superoxide dismutase activity and loss in glutamate uptake, thus compromising functional aspects of astrocytes. This platform provides a robust system to compare the temporal changes of astrocytes in the clinical markers and functional aspects of the cells at the molecular level. Our model can be utilized to investigate the intricate brain microenvironment-astrocytes signaling pathways and possibly lend to identifying new therapeutic strategies for brain injury.

ACKNOWLEDGEMENTS

CONTRIBUTIONS

S.K. and C.L.W. designed and managed the research work and improved the manuscript. C.L.W. and S.L.H. performed the experiments. S.K. and C.L.W. wrote the manuscript.

CONFLICT OF INTEREST

The authors declare no competing financial interests.

REFERENCES

1. S. A. Kruse, G. H. Rose, K. J. Glaser, A. Manduca, J. P. Felmlee, C. R. Jack, Jr. and R. L. Ehman, *NeuroImage*, 2008, **39**, 231-237.

2. J. Van Dommelen, T. Van der Sande, M. Hrapko and G. Peters, *Journal of the mechanical behavior of biomedical materials*, 2010, **3**, 158-166.

3. A. Gefen, N. Gefen, Q. Zhu, R. Raghupathi and S. S. Margulies, *Journal of neurotrauma*, 2003, **20**, 1163-1177.

4. M. C. Murphy, J. Huston, 3rd, C. R. Jack, Jr., K. J. Glaser, A. Manduca, J. P. Felmlee and R. L. Ehman, *Journal of magnetic resonance imaging : JMRI*, 2011, **34**, 494-498.

5. K. J. Streitberger, I. Sack, D. Krefting, C. Pfuller, J. Braun, F. Paul and J. Wuerfel, *PloS one*, 2012, **7**, e29888.

6. I. Sack, K. J. Streitberger, D. Krefting, F. Paul and J. Braun, *PloS one*, 2011, **6**, e23451.

7. Z. S. Xu, R. J. Lee, S. S. Chu, A. Yao, M. K. Paun, S. P. Murphy and P. D. Mourad, *Journal of Ultrasound in Medicine*, 2013, **32**, 485-494.

8. J. E. Wilk, R. K. Herrell, G. H. Wynn, L. A. Riviere and C. W. Hoge, *Psychosomatic medicine*, 2012, **74**, 249-257.

9. C. W. Hoge, D. McGurk, J. L. Thomas, A. L. Cox, C. C. Engel and C. A. Castro, *The New England journal of medicine*, 2008, **358**, 453-463.

10. D. F. Meaney and D. H. Smith, *Clinics in sports medicine*, 2011, **30**, 19-31, vii.

11. K. Dasbiswas, S. Majkut, D. E. Discher and S. A. Safran, *Nature communications*, 2015, **6**, 6085.

12. A. Buxboim, J. Swift, J. Irianto, K. R. Spinler, P. C. Dingal, A. Athirasala, Y. R. Kao, S. Cho, T. Harada, J. W. Shin and D. E. Discher, *Current biology : CB*, 2014, **24**, 1909-1917.

13. J. Swift and D. E. Discher, *Journal of cell science*, 2014, **127**, 3005-3015.

14. M. Raab, J. W. Shin and D. E. Discher, *Stem cell research & therapy*, 2010, **1**, 38.

15.   A. J. Engler, H. L. Sweeney, D. E. Discher and J. E. Schwarzbauer, *Journal of musculoskeletal & neuronal interactions*, 2007, **7**, 335.

16.   V. Natarajan, E. J. Berglund, D. X. Chen and S. Kidambi, *RSC Advances*, 2015, **5**, 80956-80966.

17.   A. Araque, G. Carmignoto, P. G. Haydon, S. H. R. Oliet, R. Robitaille and A. Volterra, *Neuron*, 2014, **81**, 728-739.

18.   A. Perez-Alvarez and A. Araque, *Current Drug Targets*, 2013, **14**, 1220-1224.

19.   A. Araque and M. Navarrete, *Philosophical transactions of the Royal Society of London. Series B, Biological sciences*, 2010, **365**, 2375-2381.

20.   A. Nimmerjahn, *The Journal of physiology*, 2009, **587**, 1639-1647.

21.   M. Belanger, I. Allaman and P. J. Magistretti, *Cell Metab*, 2011, **14**, 724-738.

22.   R. Medeiros and F. M. LaFerla, *Exp Neurol*, 2013, **239**, 133-138.

23.   M. Sidoryk-Wegrzynowicz, M. Wegrzynowicz, E. Lee, A. B. Bowman and M. Aschner, *Toxicologic pathology*, 2011, **39**, 115-123.

24.   S. K. Pirooznia, V. L. Dawson and T. M. Dawson, *Neuron*, 2014, **81**, 961-963.

25.   H. Dambach, D. Hinkerohe, N. Prochnow, M. N. Stienen, Z. Moinfar, C. G. Haase, A. Hufnagel and P. M. Faustmann, *Epilepsia*, 2014, **55**, 184-192.

26.   N. A. Oberheim, G. F. Tian, X. Han, W. Peng, T. Takano, B. Ransom and M. Nedergaard, *The Journal of neuroscience : the official journal of the Society for Neuroscience*, 2008, **28**, 3264-3276.

27.   M. V. Sofroniew, *Trends in neurosciences*, 2009, **32**, 638-647.

28.   M. Pekny and M. Nilsson, *Glia*, 2005, **50**, 427-434.

29.   L. S. Correa-Cerro and J. W. Mandell, *Journal of neuropathology and experimental neurology*, 2007, **66**, 169-176.

30.   R. J. McKeon, R. Schreiber, J. Rudge and J. Silver, *The Journal of neuroscience*, 1991, **11**, 3398-3411.

31.   B. S. Elkin, E. U. Azeloglu, K. D. Costa and B. Morrison Iii, *Journal of neurotrauma*, 2007, **24**, 812-822.

32.   I. Levental, P. C. Georges and P. A. Janmey, *Soft Matter*, 2007, **3**, 299-306.

33.   P. C. Georges, W. J. Miller, D. F. Meaney, E. S. Sawyer and P. A. Janmey, *Biophysical journal*, 2006, **90**, 3012-3018.

34.   G. M. Beaudoin III, S.-H. Lee, D. Singh, Y. Yuan, Y.-G. Ng, L. F. Reichardt and J. Arikkath, *Nature protocols*, 2012, **7**, 1741-1754.

35.   S. Kidambi, I. Lee and C. Chan, *Advanced Functional Materials*, 2008, **18**, 294-301.

36.   T. T. Tamashiro, C. L. Dalgard and K. R. Byrnes, *Journal of visualized experiments: JoVE*, 2012.

37.   R. Cole and J. de Vellis, *Protocols for neural cell culture*, 2001, 117-127.

38.   V. Natarajan, C. L. Wilson, S. L. Hayward and S. Kidambi, *PloS one*, 2015, **10**, e0134541.

39.   C. L. Wilson, V. Natarajan, S. L. Hayward, O. Khalimonchuk and S. Kidambi, *Nanoscale*, 2015, DOI: 10.1039/C5NR03646A.

40.   P. Moshayedi, L. da F Costa, A. Christ, S. P. Lacour, J. Fawcett, J. Guck and K. Franze, *Journal of Physics: Condensed Matter*, 2010, **22**, 194114.

41.   A. L. Placone, P. M. McGuiggan, D. E. Bergles, H. Guerrero-Cazares, A. Quiñones-Hinojosa and P. C. Searson, *Biomaterials*, 2015, **42**, 134-143.

42.   T. Yeung, P. C. Georges, L. A. Flanagan, B. Marg, M. Ortiz, M. Funaki, N. Zahir, W. Ming, V. Weaver and P. A. Janmey, *Cell motility and the cytoskeleton*, 2005, **60**, 24-34.

43.   S. Prauzner-Bechcicki, J. Raczkowska, E. Madej, J. Pabijan, J. Lukes, J. Sepitka, J. Rysz, K. Awsiuk, A. Bernasik and A. Budkowski, *Journal of the mechanical behavior of biomedical materials*, 2015, **41**, 13-22.

44.   J. M. Goffin, P. Pittet, G. Csucs, J. W. Lussi, J.-J. Meister and B. Hinz, *The Journal of cell biology*, 2006, **172**, 259-268.

45.   C. Eliasson, C. Sahlgren, C.-H. Berthold, J. Stakeberg, J. E. Celis, C. Betsholtz, J. E. Eriksson and M. Pekny, *Journal of Biological Chemistry*, 1999, **274**, 23996-24006.

46.   J. Qu and T. C. Jakobs, *PLoS One*, 2013, **8**, e67094.

47.   C. Lock, G. Hermans, R. Pedotti, A. Brendolan, E. Schadt, H. Garren, A. Langer-Gould, S. Strober, B. Cannella and J. Allard, *Nature medicine*, 2002, **8**, 500-508.

48.   O. A. Kolokoltsova, N. E. Yun and S. Paessler, *Virology journal*, 2014, **11**, 1.

49.   M. Pekny, *Progress in brain research*, 2001, **132**, 23-30.

50.   R. Brambilla, T. Persaud, X. Hu, S. Karmally, V. I. Shestopalov, G. Dvoriantchikova, D. Ivanov, L. Nathanson, S. R. Barnum and J. R. Bethea, *J Immunol*, 2009, **182**, 2628-2640.

51.   M. E. Hamby, J. A. Hewett and S. J. Hewett, *Glia*, 2006, **54**, 566-577.

52.   R. A. Swanson, W. Ying and T. M. Kauppinen, *Current molecular medicine*, 2004, **4**, 193-205.

53.   G. Shanker and M. Aschner, *Molecular Brain Research*, 2003, **110**, 85-91.

54.   K. J. Barnham, C. L. Masters and A. I. Bush, *Nature reviews Drug discovery*, 2004, **3**, 205-214.

55.   C. J. Weydert and J. J. Cullen, *Nature protocols*, 2010, **5**, 51-66.

56.   X. Wu, T. Kihara, A. Akaike, T. Niidome and H. Sugimoto, *Biochemical and biophysical research communications*, 2010, **393**, 514-518.

57.   J. L. Ridet, S. K. Malhotra, A. Privat and F. H. Gage, *Trends in neurosciences*, 1997, **20**, 570-577.

58.   M. Eddleston and L. Mucke, *Neuroscience*, 1993, **54**, 15-36.

59.   W. T. Norton, D. A. Aquino, I. Hozumi, F. C. Chiu and C. F. Brosnan, *Neurochemical research*, 1992, **17**, 877-885.

60.   B. MORRISON III, K. E. SAATMAN, D. F. MEANEY and T. K. McINTOSH, *Journal of neurotrauma*, 1998, **15**, 911-928.

61.   L. F. Eng, A. C. Yu and Y. L. Lee, *Progress in brain research*, 1992, **94**, 353-365.

62.   W. J. Miller, I. Leventhal, D. Scarsella, P. G. Haydon, P. Janmey and D. F. Meaney, *Journal of neurotrauma*, 2009, **26**, 789-797.

63.   A. C. H. Yu, B. Y. Wu, R. Y. Liu, Q. Li, Y. X. Li, P.-F. Wong, S. Liu, L. T. Lau and Y. W. W. Fung, *Neurochemical research*, 2004, **29**, 2171-2176.

64.   Y. J. Hou, A. C. Yu, J. M. Garcia, A. Aotaki-Keen, Y. L. Lee, L. F. Eng, L. J. Hjelmeland and V. K. Menon, *Journal of neuroscience research*, 1995, **40**, 359-370.

65.   P. Yu, H. Wang, Y. Katagiri and H. M. Geller, *Methods Mol Biol*, 2012, **814**, 327-340.

66.   K. Miller, K. Chinzei, G. Orssengo and P. Bednarz, *Journal of biomechanics*, 2000, **33**, 1369-1376.

67.   A. Arani, M. C. Murphy, K. J. Glaser, A. Manduca, D. S. Lake, S. A. Kruse, C. R. Jack, Jr., R. L. Ehman and J. Huston, 3rd, *Neuroimage*, 2015, **111**, 59-64.

68.   M. J. Paszek, N. Zahir, K. R. Johnson, J. N. Lakins, G. I. Rozenberg, A. Gefen, C. A. Reinhart-King, S. S. Margulies, M. Dembo and D. Boettiger, *Cancer cell*, 2005, **8**, 241-254.

69.   G. M. Ribbers, *Retrieved November*, 2008, **8**, 2012.

70.   M. Prager-Khoutorsky, A. Lichtenstein, R. Krishnan, K. Rajendran, A. Mayo, Z. Kam, B. Geiger and A. D. Bershadsky, *Nature cell biology*, 2011, **13**, 1457-1465.

71.   Y.-B. Lu, I. Iandiev, M. Hollborn, N. Körber, E. Ulbricht, P. G. Hirrlinger, T. Pannicke, E.-Q. Wei, A. Bringmann and H. Wolburg, *The FASEB Journal*, 2011, **25**, 624-631.

72.   P. Yu, H. Wang, Y. Katagiri and H. M. Geller, in *Astrocytes*, Springer, 2012, pp. 327-340.

73.   X. Jiang, P. C. Georges, B. Li, Y. Du, M. K. Kutzing, M. L. Previtera, N. A. Langrana and B. L. Firestein, *The Open Neuroscience Journal*, 2007, **1**, 7-14.

74.   M. L. Previtera, C. G. Langhammer and B. L. Firestein, *Journal of bioscience and bioengineering*, 2010, **110**, 459-470.

List of Figures

Figure 1: Schematic of experimental design. Primary rat astrocytes were isolated from Day 1-3 rat pups. Culture purity was determined to be >90% GFAP positive cells by immunocytochemistry. Cells were seeded on PLL coated Cytosoft® 6 well plates with physiologically relevant stiffness (200 Pa/soft mimics healthy brain tissue and 8000 Pa/stiff mimics diseased/injured brain tissue). After three days in culture, the phenotypic markers and changes in morphology of primary astrocytes were assessed to demonstrate astrogliosis like behavior in astrocytes when cultured on stiff substrates. Scale bar 100 μm. Figure drawn by Christina L Wilson.

Figure 2: Change in cell morphology reveals activation on soft (200 Pa) vs stiff (8000 Pa) surfaces. (A) Representative images of astrocyte morphology visualized with actin staining . White arrow indicates distinct actin stress fibers not seen on the soft surface. Scale bar 100 μm. (B) Cell size and (C) circularity quantification of actin images utilized NIH Image J. N = 4, "*" indicates $P < 0.05$.

Figure 3: Culture on stiff substrate induces increase in cell proliferation and up-regulation of astrogliosis markers. (A) Quantification of BrdU incorporation by flow cytometry N = 3. (B) Quantification of GFAP and Vimentin protein expression, N = 4 or 5. "*" $P < 0.05$.
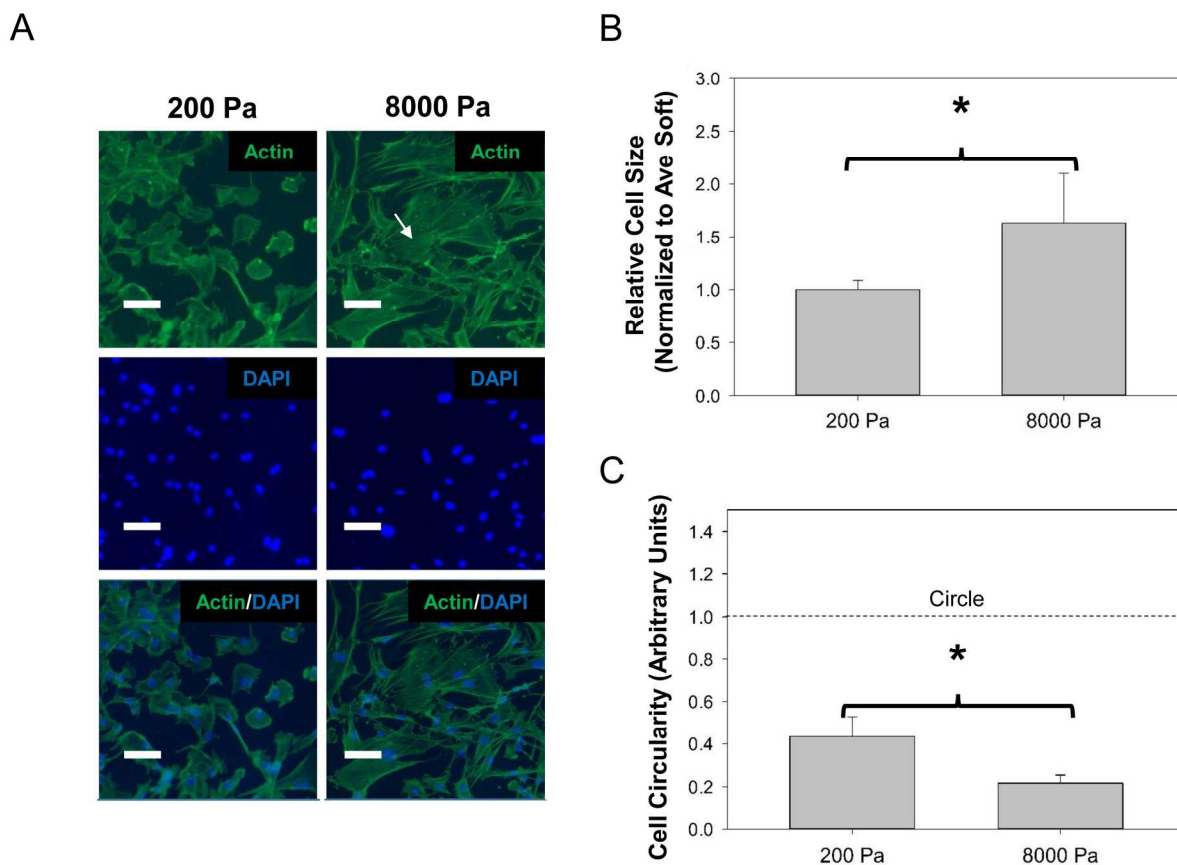
Figure 4: Culture on stiff substrate results in generation of ROS in primary astrocytes. (A) Quantification of ROS generation using H_2DCFDA based fluorescence assay and flow cytometry, N = 3. (B) Quantification of CuZnSOD by in gel activity assay, N = 3 or 4. "*" indicates $P < 0.05$ and "**" indicates $P < 0.001$.

Figure 5: Effect of stiff substrates on glutamate uptake. (A) Glutamate uptake of radiolabeled glutamate by astrocytes on soft and stiff surfaces. (B) RT-PCR gene expression quantification of glutamate transporters, GLAST and GLT1, on soft and stiff surfaces, N = 3. (C) Western blot quantification of protein expression of glutamate transporters, GLT1 and GLAST, on soft and stiff surfaces, N = 4.   "*" $P<0.05$.

Figure 6: Schematic overview. By culturing on 200 and 8000 Pa PDMS culture surfaces primary astrocytes become activated on the stiff surface with changed morphology, increased proliferation and increased GFAP protein expression. In the reactive phenotype induced by surface culture stiffness astrocytes exhibit increased ROS, increased CuZnSOD activity and decreased glutamate uptake similar to reactive astrocytes in vivo.
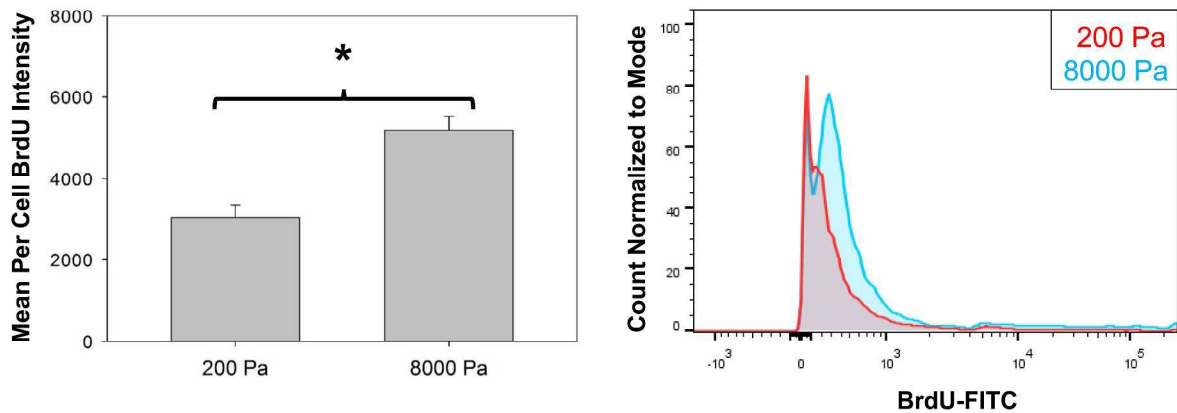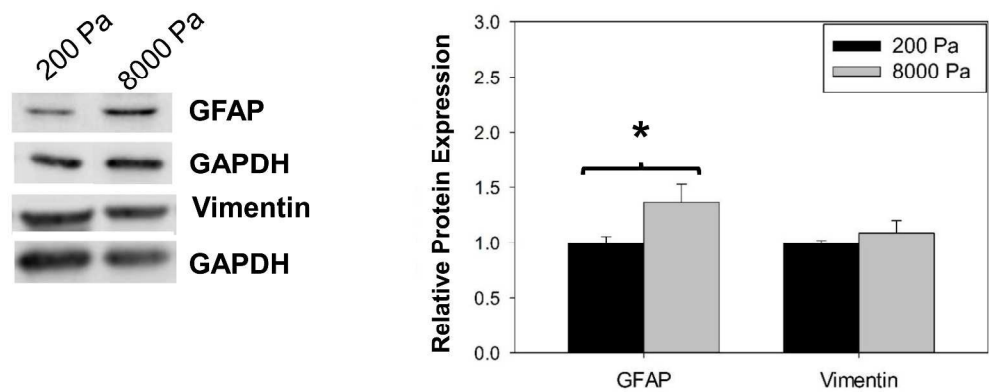
Figure 1: Schematic of experimental design. Primary rat astrocytes were isolated from Day 1-3 rat pups. Culture purity was determined to be >90% GFAP positive cells by immunocytochemistry. Cells were seeded on PLL coated Cytosoft® 6 well plates with physiologically relevant stiffness (200 Pa/soft mimics healthy brain tissue and 8000 Pa/stiff mimics diseased/injured brain tissue). After three days in culture, the phenotypic markers and changes in morphology of primary astrocytes were assessed to demonstrate astrogliosis like behavior in astrocytes when cultured on stiff substrates. Scale bar 100 μm. Figure drawn by Christina L Wilson.

A

8000 Pa   200 Pa

Figure 2: Change in cell morphology reveals activation on soft (200 Pa) vs stiff (8000 Pa) surfaces. (A) Representative images of astrocyte morphology visualized with actin staining (A). White arrow indicates distinct actin stress fibers not seen on the soft surface. Scale bar 100 μm. Cell size (B) and circularity (C) quantification of actin images utilized NIH Image J. N = 4, "*" indicates $P < 0.05$.
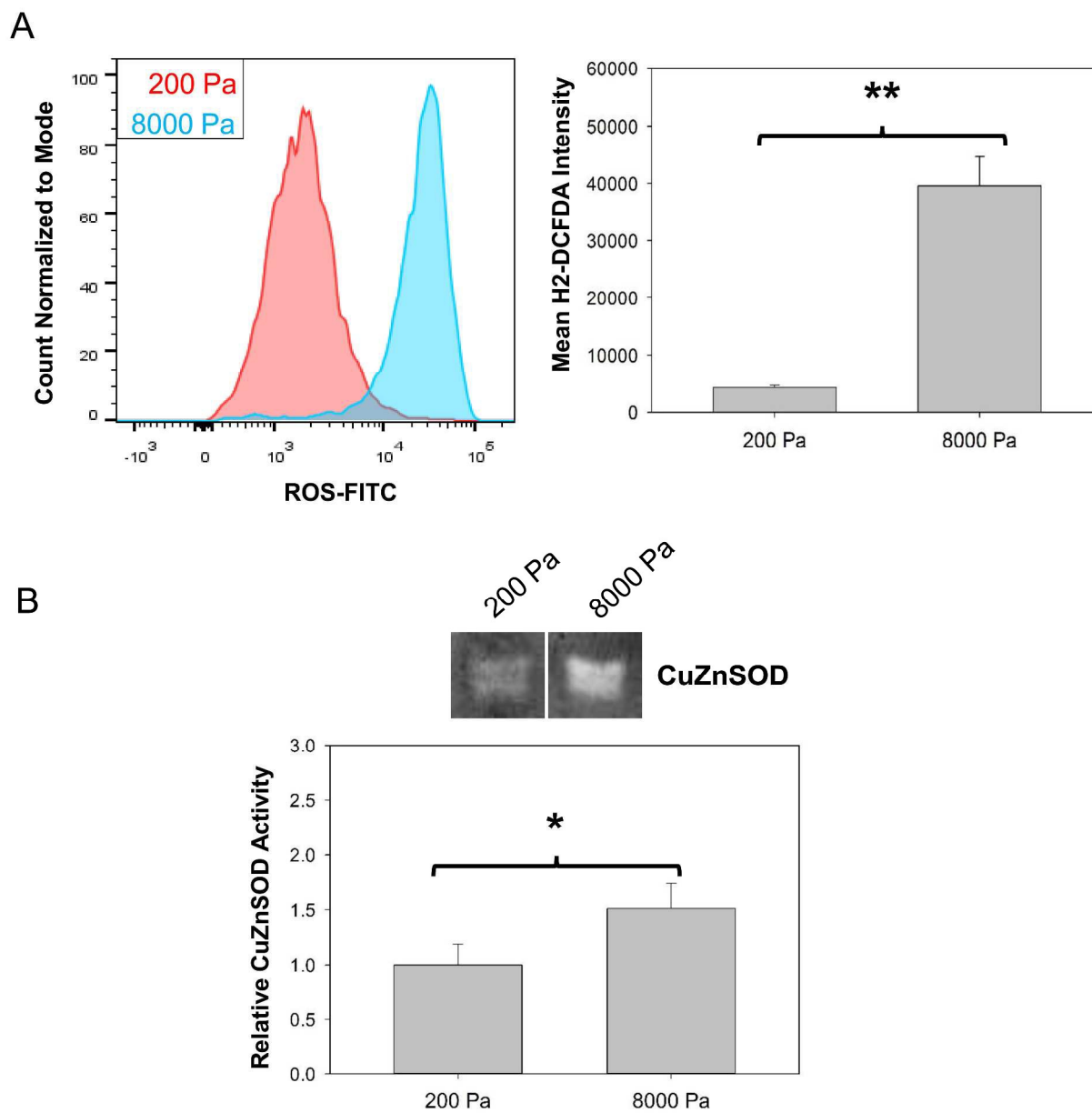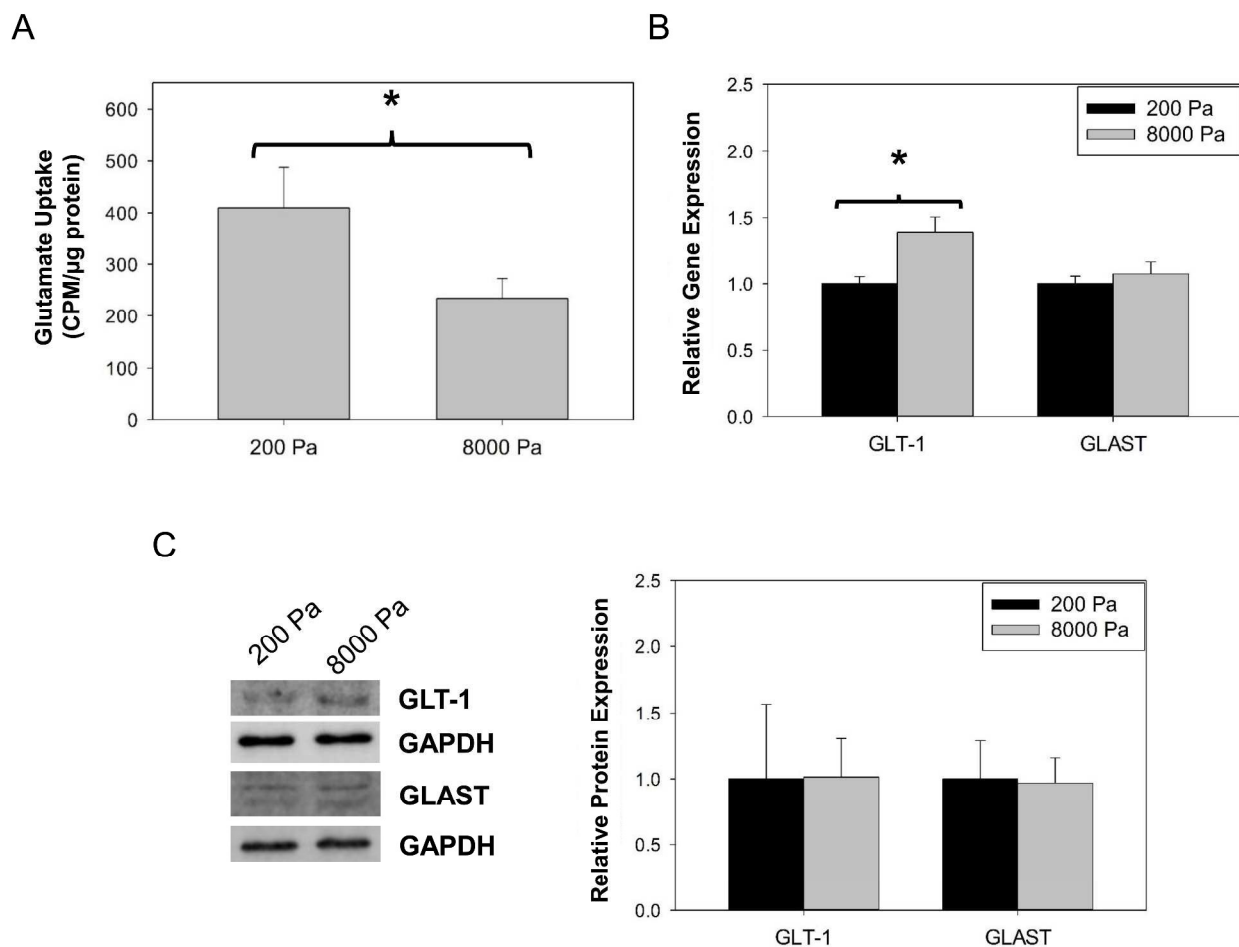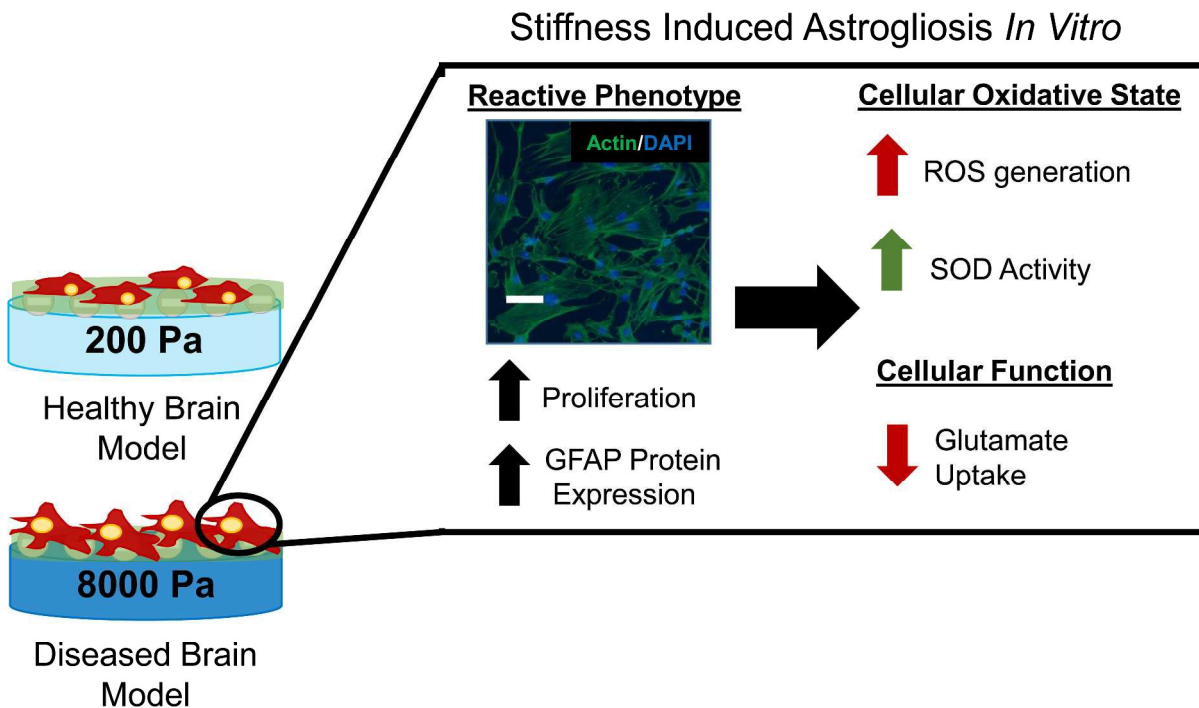
A

B

Figure 3: Culture on stiff substrate induces increase in cell proliferation and up-regulation of astrogliosis markers. (A) Quantification of BrdU incorporation by flow cytometry N = 3. (B) Quantification of GFAP and Vimentin protein expression, N = 4 or 5. "*" P < 0.05.
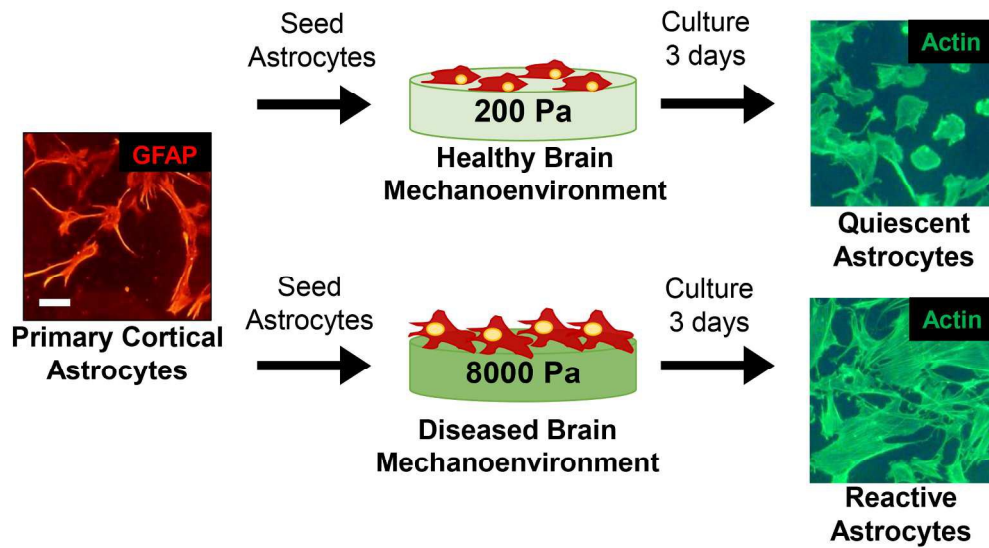
Figure 4: Culture on stiff substrate results in generation of ROS in primary astrocytes. (A) Quantification of ROS generation using H₂DCFDA based fluorescence assay and flow cytometry, N = 3. (B) Quantification of CuZnSOD by in gel activity assay, N = 3 or 4. "*" indicates $P < 0.05$ and "**" indicates $P < 0.001$.

Figure 5: Effect of stiff substrates on glutamate uptake. (A) Glutamate uptake of radiolabeled glutamate by astrocytes on soft and stiff surfaces. (B) RT-PCR gene expression quantification of glutamate transporters, GLAST and GLT1, on soft and stiff surfaces, N = 3. (C) Western blot quantification of protein expression of glutamate transporters, GLT1 and GLAST, on soft and stiff surfaces, N = 4.   "*" P<0.05.

Figure 6: Schematic overview. By culturing on 200 and 8000 Pa PDMS culture surfaces primary astrocytes become activated on the stiff surface with changed morphology, increased proliferation and increased GFAP protein expression. In the reactive phenotype induced by surface culture stiffness astrocytes exhibit increased ROS, increased CuZnSOD activity and decreased glutamate uptake similar to reactive astrocytes in vivo.

205x112mm (300 x 300 DPI)